Published in final edited form as:
Nucl Med Biol. 2007 May ; 34(4): 353–361.

PET Imaging of CRF1 with [^{11}C]R121920 and [^{11}C]DMP696: Is the Target of Sufficient Density?

Gregory M. Sullivan[a], **Ramin V. Parsey**[a], **J. S. Dileep Kumar**[a], **Victoria Arango**[a], **Suham A. Kassir**[a], **Yung-yu Huang**[a], **Norman R. Simpson**[a], **Ronald L. Van Heertum**[a], and **J. John Mann**[a,b]

aDepartment of Psychiatry and Division of Neuroscience, Columbia University and the New York State Psychiatric Institute, 1051 Riverside Drive, New York, NY 10032, USA

bDepartment of Radiology, Columbia University, New York, NY 10032, USA

Abstract

Aim—Overstimulation of the CRF type 1 receptor (CRF1) is implicated in anxiety and depressive disorders. The aim of this study was to investigate the in vivo binding characteristics of [^{11}C]R121920 and [^{11}C]DMP696 in the non-human primate for application in positron emission tomography (PET) studies of CRF1.

Methods—PET imaging with the two novel CRF1 radioligands was performed in baboon. In vitro binding studies for CRF1 were performed in postmortem brain tissue of baboon and human to assess sufficiency of receptor density for PET.

Results—Both [^{11}C]R121920 and [^{11}C]DMP696 distributed rapidly and uniformly throughout brain. Washout was comparable across brain regions, without differences in volume of distribution between regions reported to have high and low in vitro CRF1 binding. Membrane-enriched tissue homogenate assay using [^{125}I]Tyr^{0}-sauvagine and specific CRF1 antagonists CP154,526 and SN003 in human occipital cortex yielded maximal binding (B_{max}) of 63.3 and 147.3 fmol/mg protein, respectively, and in human cerebellar cortex yielded B_{max} of 103.6 and 64.6 fmol/mg protein, respectively. Dissociation constants (K_D) were subnanomolar. In baboon, specific binding was not detectable in the same regions; therefore B_{max} and K_D were not measurable. Autoradiographic results were consistent except there was also detectable CRF1-specific binding in baboon cerebellum.

Conclusion—Neither [^{11}C]R121920 nor [^{11}C]DMP696 demonstrated quantifiable regional binding in vivo in baboon. In vitro results suggest CRF1 density in baboon may be insufficient for PET. Studies in man may generate more promising results due to the higher CRF1 density compared with baboon in cerebral cortex and cerebellum.

Keywords

corticotropin-releasing factor (CRF); positron emission tomography (PET); R121220; DMP696; SN003; baboon; radioligand

*__Corresponding Author:__ Gregory M. Sullivan, M.D., Division of Neuroscience, Department of Psychiatry, Columbia University College of Physicians & Surgeons, 1051 Riverside Drive, Unit #41, New York, NY 10032, Phone: 212 543-6760, Facsimile: 212 543-5437, Email: gms11@columbia.edu

1. Introduction

Corticotropin-releasing factor (CRF) is a 41-amino acid peptide, first isolated from hypothalamus, that was shown to activate the hypothalamic-pituitary-adrenal (HPA) axis by stimulating release of adrenocorticotropic hormone (ACTH) by the pituitary [1]. CRF is present in widespread brain regions and is a central mediator of the behavioral, autonomic, endocrine, and immune responses to stress [2]. The physiological effects of CRF are mediated by at least two G-protein coupled receptors, CRF1 and CRF2 [3]. CRF also binds to CRF-binding protein (CRF-BP), a membrane-associated protein that regulates local availability of CRF at its receptors [4].

Rodent studies indicate that the CRF1 and CRF2 receptors are pharmacologically distinct and have different anatomical distributions [5]. In the rodent, CRF1 mediates effects on the HPA axis and anxiety-related behaviors [6] and CRF2 affects feeding behaviors [7]. There are important species differences in the distributions of mRNA and protein of these two receptors between non-human primate and rodent [8,9]. In pituitary, CRF1 protein level depends on post-transcriptional regulatory mechanisms [10] suggesting dissociation of protein density from mRNA level for this receptor.

CRF hypersecretion is implicated in the pathogenesis of mood and anxiety disorders. Higher CRF in cerebrospinal fluid (CSF) has been reported in major depression [11–13], as well as PTSD [14], Tourette's syndrome [15], anorexia nervosa [16], and suicide [17–20]. Postmortem studies of suicides report higher pontine [21] and frontal cortical [22] CRF peptide, and lower frontal cortical CRF binding sites [23] and CRF1 mRNA [22]. CRF1 antagonists are in development as potential therapeutic agents in mood and anxiety disorders [24,25]. The CRF1 antagonist R121919 reduces anxiety-related behaviors in rodent [6,26], and anxiolytic and antidepressant effects are suggested in man [27].

A positron emission tomography (PET) radioligand for CRF1 would permit *in vivo* quantification of regional brain binding in psychiatric disorders and suicidal behaviors as well as receptor occupancy relationships for therapeutic drug studies. There have been only a few reports on the development of CRF1 radioligands for PET or single photon emission tomography (SPECT) imaging. Using the high affinity, selective, nonpeptide CRF1 antagonist antalarmin (*N*-butyl-*N*-ethyl[2,5,6-trimethyl-7-(2,4,6-trimethylphenyl)pyrrolo-[2,3-*d*] pyrimidin-4-yl]-amine; K_i=2.5 nM) as a template, several fluoro-substituted analogues were synthesized [28]. One with subnanomolar affinity for CRF1 (K_i=0.91 nM) proved to have poor penetration of the blood-brain barrier (BBB), prompting the design of more hydrophilic analogues with calculated log P values (ClogP) less than that of antalarmin (ClogP=7.0) [29]. An iodinated analogue for SPECT imaging was successfully converted to a targeted I-125 pure product, but, unfortunately, it also had reduced affinity (K_i=14 nM) for CRF1 [30]. Fluorinated and iodinated derivatives based on the high affinity CRF1 antagonist CP-154,526 (K_i=0.48 nM) have also been synthesized. Two with subnanomolar binding affinities (K_i=0.52 nM, 0.94 nM) were radiolabeled with F-18 and I-123, respectively [31]. Yet, in rodent both showed low accumulation in brain and very poor uptake and retention in regions of high CRF1 density. More recently, a high affinity (K_i=1.9 nM), lower lipophilicity (ClogP=3.05) brominated derivative of CP-154,526 was synthesized and labeled with Br-76 [32]. Biodistribution studies in rat indicated [^{76}Br]MJL-1-109-2 crosses the BBB, and autoradiography demonstrated a pattern of CRF1 specific binding comparable with the known distribution of CRF1. Yet, to date, testing in PET has not been reported.

We have previously reported on a potential CRF1 radioligand [^{11}C]SN003 [33]. We now report on two new small molecule CRF1 antagonist ligands that are candidates for PET imaging, R121920 and DMP969, that we have labeled with carbon-11 and tested for in vivo binding in

baboon. Since one of the essential criteria for the success of a PET radioligand is sufficient density of the target protein [34], we also performed membrane-enriched tissue homogenate and autoradiographic binding studies of CRF1 in baboon and human brain to determine if CRF1 protein density is sufficient for PET.

2. Materials and methods

2.1. Synthesis of [^{11}C]R121920 and [^{11}C]DMP696

The methodologies for the preparation of precursors and the radiosyntheses for [^{11}C]R121919 and [^{11}C]DMP696 have been described previously [35,36]. Table 1 shows the molecular weights (MW), melting points (MP), partition coefficients (log$P_{o/w}$), and K_i for the these ligands along with synthesis time, radiochemical yield, purity, and specific activity (SA). Our previously reported CRF1 radioligand, [^{11}C]SN003 [33], is included in the table for comparison purposes. Figure 1 shows the chemical structures of all three radioligands for CRF1.

2.2. PET imaging in baboon

Experiments were carried out in accordance with a protocol approved by the Columbia University Medical Center and New York State Psychiatric Institute Animal Care Committees and government regulations. Two male baboons (*Papio anubis*), studied in a fasted state, were utilized. Six PET scans for [^{11}C]DMP696 (mean injected dose, 3.48 mCi; mean SA, 2.86 Ci/micromole) and four scans for [^{11}C]R121920 (mean injected dose, 1.75 mCi; mean SA, 3.77 Ci/micromole) were performed using an ECAT EXACT HR+ scanner (Siemens/CTI, Knoxville, TN). The baboons were immobilized with ketamine (10 mg/kg, intramuscular) and anesthetized with isoflurane 1.5–2% (via endotracheal tube) general anesthesia. Physiological conditions (heart rate, blood pressure, respiration, blood gases/pH, O_2 saturation) were monitored and maintained during each scan by mechanical ventilation, endotracheal anesthesia, and intravenous (i.v.) fluids (0.9% NaCl). Core temperature was maintained at 37 °C by use of a heated water blanket. A 10-min transmission scan was obtained using a ^{68}Ge rotating rod source. Radiotracer was injected by i.v. bolus, and emission data were collected for 120 min in 3-D mode with the following frame times: 2 × 0.5 min, 3 × 1 min, 5 × 2 min, 4 × 4 min, and 9 × 10 min. Plasma activity from arterial samples collected at regular intervals was measured in a well counter (Wallac 1480 Wizard 3M Automatic Gamma Counter, PerkinElmer, Boston, MA). The percentage of radioactivity in plasma due to unmetabolized parent radioligand was determined for six plasma samples obtained at different times as previously described [37].

2.3. PET image processing

Magnetic resonance image (MRI) scans were acquired for each baboon, and regions of interest were drawn on the MRI. PET data was reconstructed with attenuation correction using the transmission data, and scatter correction was performed. PET images were realigned to the MRI using Automated Image Registration (AIR) algorithm [38,39]. Regions of interest were transferred to the PET images, and time-activity curves were generated using the measured activity of each ROI. Right and left regions were averaged.

The distribution volume (V_T) of a radiotracer in a tissue is the volume of the tissue in which the tracer would have to distribute to reach a concentration equal to that in plasma. Regional V_T was calculated for each ROI using the likelihood estimation in graphical analysis (LEGA) approach [40], which estimates the parameters using standard likelihood theory. Brain activity was corrected for the contribution from the cerebrovasculature by assuming a 5% blood volume in the ROIs [41]. V_T (ml of plasma/g of tissue) is defined as the ratio of the tracer concentration in the region of interest to the metabolite-corrected plasma concentration of the tracer at

"equilibrium", noting that true equilibrium is not achieved in dynamic modeling of receptor density using PET with short-lived positron emitters [41,42]. V_T represents the sum of the free and nonspecifically bound distribution volume (V_2) and the specifically bound distribution volume (V_3). A four parameter logistic function was used to fit the metabolite data to a curve. The time to 50% of the parent remaining in arterial blood was extrapolated from the metabolite curves for each of the radioligands.

2.4. Brain tissue sources for in vitro binding studies in human and baboon

Postmortem human brain tissue in this study came from control subjects determined to be without psychiatric disease or neurological disease and in whom toxicological analysis of brain tissue and body fluids was negative for the presence of psychotropic medications or drugs of abuse. The postmortem delay of each of the chosen cases was less than 16 hours. Postmortem human and baboon brains were collected at autopsy, sectioned in coronal blocks, frozen in Freon, and stored at −80°C until dissection for membrane-enriched tissue homogenate binding or frozen sectioning at 20 μm for autoradiography. Dissected tissue from both human and baboon brains was adjacent to slices used for autoradiography. Endogenous ligand was removed by the repeated washing steps for the membrane-enriched tissue homogenate binding assay and by the preincubation step for the autoradiography.

2.5. Membrane-enriched brain tissue homogenate binding assay

[^{125}I]Tyr^0-sauvagine (PerkinElmer, Wellesley, MA; SA, 2200 Ci/mmol) binding to human and baboon occipital cortex and cerebellar tissue homogenates was assayed essentially as described by Rominger et al [43]. Briefly, tissue samples from occipital cortex and cerebellum were homogenized in 10X of buffer A (pH 7.2; 50 mM HEPES, 10 mM $MgCl_2$, 2 mM EGTA and 1 μg/ml each of the peptidase inhibitors aprotinin, leupeptin and pepstatin) at 4°C using a POLYTRON homogenizer (Brinkmann, Westbury, NY; setting 4) for 10 s. The tissue homogenate was centrifuged at 20,000 × *g* for 15 min. The resulting pellet was washed by repeating the homogenization and centrifugation steps two additional times. The final membrane-enriched pellet was resuspended in buffer A, and the suspension was diluted using binding assay buffer B (50 mM HEPES, pH 7.7; 10 mM $MgCl_2$; 2 mM EGTA; 0.1% BSA) to final concentration of 0.2 mg protein/ml, as assayed by the BCA Protein Assay (Pierce, Rockford, IL).

[^{125}I]Tyr^0-sauvagine binding assays were carried out in duplicate in 5 ml plastic tubes. Total assay volume was 200 μl. Nonspecific binding was defined in the presence of CP154,526 (2 μM) or SN003 (5 μM) or ovine CRF (oCRF; 2 μM). The reaction mixture consisted of 100 μl homogenate, 50 μl [^{125}I]Tyr^0-sauvagine, and 50 μl of buffer or CP154,526 or SN003 or oCRF. After 2 h incubation at room temperature, incubation was terminated by the addition of 5 ml ice-cold buffer B to each tube, and the contents were filtered using a Brandell cell harvester (M-24RI; Gaithersburg, MD) under reduced pressure through Whatman GF/B glass fiber filters (Florham Park, NJ) pre-treated with 1.0% ethylene imine polymer solution (Fluka, Buchs, Switzerland) and presoaked with ice-cold 50 mM HEPES washing solution. Filters were air-dried and transferred into 5 ml Falcon plastic tube (Becton Dickinson, Bedford, MA) for activity measurement in a Cobra II gamma counter (PerkinElmer Life Sciences, Downers Grove, IL).

Saturation studies were performed over a concentration range of 0.02 to 0.25 nM of [^{125}I] Tyr^0-sauvagine. Specific binding was calculated by subtracting the nonspecific binding from total binding, and linear conversion of the specific association data was performed. Data were fitted to a one-site binding model using EDBA software (EBDA/LIGAND written by G.A. McPherson; Biosoft-Elsevier, Cambridge, UK) for determination of the maximal number of binding sites (B_{max}) and the apparent dissociation constant (K_D).

2.6. Autoradiographical analysis

Methods for in vitro CRF1 binding autoradiography in post-mortem human brain samples were adapted from three reports [9,44,45]. Human and baboon brain sections cut at 20-μm thick were pre-incubated for 30 min at 23° C in 50 mM HEPES buffer (pH 7.2) containing 10 mM $MgCl_2$, 2 mM EGTA, 100 mM KIU/ml aprotinin, 0.1 mM bacitracin, 0.1 mM ovalbumin. Sections were incubated in the same solution but also containing 0.150 nM [^{125}I]Tyr^0-sauvagine for 2 h at 23° C. Parallel incubation of adjacent sections with CP154,526 (1 μM) or SN003 (1 μM) in the incubation solution was carried out to allow determination of nonspecific binding. Following incubation, sections were washed twice at 4° C for 5 min per wash in phosphate buffered saline with 0.01% Triton X-100 followed by a dip in ice cold distilled H_2O. Sections were dried under a stream of cold air and then placed in a desiccator until completely dry. Sections were exposed to Kodak Biomax MR film for 2–3 days and then developed using Kodak D-19 developer and digitally scanned.

3. Results

3.1. Metabolism of [^{11}C]R121920 and [^{11}C]DMP696 in baboon

Both [^{11}C]R121920 and [^{11}C]DMP696 were rapidly metabolized, with mean times to 50% of parent ligand remaining in plasma of 12.9 min for [^{11}C]R121920 and 9.2 min for [^{11}C] DMP696. Figure 2A & Figure 2B show the remaining percentage of unmetabolized parent compound for the two radioligands as a function of time.

3.2. PET imaging in baboon

Both [^{11}C]R121920 and [^{11}C]DMP696 demonstrated a pattern of distribution consistent with BBB penetration and early accumulation of the parent compound in the brain. Representative time-activity curves for [^{11}C]R121920 and [^{11}C]DMP696 are presented in Figure 3A & Figure 3B. No brain region had detectable specific binding, with nearly identical time-activity curves for regions known to have higher (cerebellum, occipital cortex) and lower (putamen) CRF1 receptor density reported for primates in the literature [9,46,47]. Likewise, no brain region demonstrated evidence for detectable specific binding of any radiolabeled metabolite of these radiotracers. Figure 4B–Figure 4D show voxel V_T brain maps for [^{11}C]R121920, [^{11}C] DMP696, and our previously reported CRF1 radioligand, [^{11}C]SN003. Table 2 shows mean V_T values for these CRF1 radioligands for ROIs with known lower (putamen) and higher (cerebellum, occipital cortex) CRF1 binding. Although no pattern of specific binding is evident for any of the three radioligands, the V_T across brain regions is largest for [^{11}C]DMP696 and smallest for [^{11}C]R121920.

3.3. Membrane-enriched brain tissue homogenate binding assay

The B_{max} for CRF1 was calculated for two brain regions from human brain and baboon brain. Displacement of [^{125}I]Tyr^0-sauvagine using specific CRF1 antagonists CP154,526 (2 μM) and SN003 (5 μM) in human occipital cortex yielded B_{max} of 63.3 and 147.3 fmol/mg protein, respectively, and in cerebellar cortex yielded B_{max} of 103.6 and 64.6 fmol/mg protein, respectively. In contrast, in baboon displacement of [^{125}I]Tyr^0-sauvagine using the same blocking concentrations of CP154,526 and SN003 and conducting the assays in the same batch, the B_{max} in occipital cortex and cerebellar cortex was undetectable. The calculated K_D^S were subnanomolar for the CRF1 receptor in human brain, with K_D^S of 0.014 nM for human occipital cortex and 0.028 nM for human cerebellum using CP154,526 for displacement. The K_D^S were not measurable in baboon brain. A third blocking agent, oCRF was also used to displace [^{125}I]Tyr^0-sauvagine binding. This peptide has affinity for CRF1, CRF2 and CRF binding protein. Using oCRF, B_{max} was 301 and 182.9 fmol/mg protein for human occipital cortex and

human cerebellar cortex, respectively. In baboon, B_{max} was 117.5 and 90.9 fmol/mg protein in occipital and cerebellar cortex, respectively, using oCRF for blocking.

3.4. Autoradiographical analysis

Autoradiography using [^{125}I]Tyr^{0}-sauvagine and CP154,526 or SN003 was performed to determine qualitatively if there is visually-detectable specific binding to the CRF1 receptor in two regions selected for detectable CRF1 receptor binding in primates as previously reported [9,47]. Representative sections (see Fig. 5A–Fig. 5I) of occipital cortex from human and cerebellum from both human and baboon demonstrate [^{125}I]Tyr^{0}-sauvagine binding and specific displacement from the CRF1 receptor by the CRF1-specific antagonists CP154,526 (1 μM) and SN003 (1 μM). These results are consistent with the saturation binding isotherms in membrane preparations reported above. Additionally, there is visually-detectable CRF1-specific binding in baboon cerebellum (see 5C, 5F, and 5I) by autoradiography, albeit less than in human cerebellum.

4. Discussion

We report on the development of two novel C-11 CRF1 radioligands, [^{11}C]R121920 and [^{11}C]DMP696, for PET imaging. However, similar to our prior report of the CRF1 radioligand [^{11}C]SN003 [33], in vivo testing of these ligands failed to demonstrate detectable specific binding in baboon brain using PET. The imaging analyses included several brain regions known to contain significant levels of the CRF1 receptor in primate such as cerebellum and multiple cortical regions [9,46,47]. The distribution pattern of radioactivity throughout brain demonstrated by the time-activity curves indicated these radioligands penetrate the BBB and accumulate in brain tissue. But all regions have a similar washout pattern, without evidence of specific CRF1 binding signal in regions known to have greater expression of CRF1 receptors. If this failure to identify specific binding is due to particular characteristics of the individual radioligands, future development of other CRF1 radioligands should proceed. Yet, one of the essential criteria for the success of a PET radioligand is sufficient density of the target protein [34]. It is possible that the density of CRF1 in baboon brain is insufficient for imaging by PET, and this could explain the absence of identifiable specific binding of these radioligands. To address this possibility, we also conducted an *in vitro* survey of CRF1 density in selected regions in baboon and human brain. We utilized both a quantitative membrane-enriched tissue homogenate assay and qualitative autoradiography to address this question.

There is a paucity of published data characterizing regional receptor density of CRF1 in brain in man or non-human primate, perhaps indicative of a relatively low density in most brain regions. In an early report, Millan et al surveyed CRF binding in cynomolgus monkeys utilizing 0.2 nM [^{125}I]-ovineCRF (oCRF) in a membrane-enriched tissue homogenate assay. Nonspecific binding was determined in the presence of 1 μM of unlabeled oCRF. They reported concentrations of CRF binding sites from cingulate cortex, amygdala, and hippocampus of 138 ±9, 150±7, and 47±11 fmol/mg, respectively [46]. Because oCRF is reported to bind both CRF1 and CRF2, the reported specific binding concentrations by Millan et al may reflect binding to CRF1 and CRF2. On the other hand, it is reported that oCRF is relatively specific for CRF1 at a concentration of 100 nM [48], so the concentration of radiolabeled oCRF employed may have allowed determination of specific binding for CRF1. The value of binding in cingulate is similar to our findings for occipital cortex in baboon and man.

Nemeroff et al [23] reported on the maximal number and affinity of CRF binding sites in post-mortem membrane-enriched tissue homogenates from frontal pole (Brodmann's areas 10 and 11) of 26 suicides and 29 controls. Using 0.05 nM [^{125}I]-oCRF and displacement with unlabeled rat/human CRF at concentrations ranging from 125 pM to 0.5 μM, they reported a B_{max} of 521±43 fmol/mg protein in the suicides which was lower than that of controls at 680

±51 fmol/mg protein. There was no difference in K_D between groups. Our finding of 63.3 fmol/mg protein for B_{max} in human occipital cortex, using CP154,526 for CRF1-specific displacement, is one order of magnitude lower than the mean reported for controls by Nemeroff et al. It is notable that our assays differed considerably, as we utilized [^{125}I]Tyr^0-sauvagine and varying concentrations of unlabeled sauvagine. It may be the case that the reported specific binding by Nemeroff et al reflected not only CRF1 binding but also binding to CRF2 and CRF-binding protein. Performing our same tissue membrane homogenate assay for baboon brain under the same conditions and in the same batch as for human brain, specific CRF1 binding was not detectable when using either of the highly specific CRF1 antagonists CP154,526 and SN003 as the specific displacers (although our autoradiography indicated a low level of detectable binding in baboon cerebellum). This is consistent with our PET imaging findings with CRF1 radioligands in baboon in which we failed to identify specific binding.

Similar to our autoradiographic studies, Sanchez et al [9] determined relative CRF1 densities in the rhesus macaque using [^{125}I]Tyr^0-sauvagine with and without the specific CRF1 antagonist CP154,526. Highest binding was identified in pituitary followed by particular amygdala nuclei (paralaminar, accessory basal, lateral); the granular layer of cerebellum; dentate gyrus; layers I–V of entorhinal, insular, and cingulate cortex; and medial PFC. No detectable CRF1 protein binding was found in regions that included CA1, CA2, and CA3 of hippocampus, BNST, raphe nuclei, and choroid plexus. Our limited regional sampling with autoradiographic and membrane-enriched tissue homogenate assays using CP154,526 was consistent with the data of Sanchez et al in that cerebellum showed greater CRF1 specific binding than cortex. It should be noted that although the pituitary has been repeatedly shown to have the highest CRF1 binding in multiple species, there are a number of factors making reliable estimates of binding by PET difficult, if not impossible, for pituitary. Such factors include difficulty in localization and ROI placement, partial volume effects, proximity of [high flow rate] portal blood supply, and scatter/noise due to bone surrounding the pituitary fossa.

It is important to point out that several factors other than the in vivo B_{max} and K_D may adversely affect the ability to detect specific binding of a PET radioligand to CRF1. The activity due to specific binding must be greater than background activity, including the background activity due to nonspecific binding. Ideally, no radiolabeled metabolites should enter brain, and non-radiolabeled metabolites that enter brain should not bind to the target. We did not see evidence of radiolabeled metabolites in brain with these radioligands, at least to the degree that the time-activity curves did not evidence differential retention of any radiolabeled molecule. As well, release of endogenous ligand, in this case CRF, may alter binding and dissociation of nonpeptide antagonists for CRF1 [49]. Therefore, a stress response in the baboons due to preparation for PET imaging might be of particular relevance for detection of CRF1 given the receptor's central role in the stress response system. As well, the effects of ketamine preanesthetic and the isoflurane anesthesia must be considered, particularly given recent work suggesting isoflurane anesthesia alters brain to plasma distribution ratios of the 5-HT$_{1A}$ antagonist radioligand [^{18}F]FPWAY [50].

5. Conclusion

In summary, we report on two new C-11 radioligands for CRF1 and PET, [^{11}C]DMP696 and [^{11}C]R121920. Like our prior finding with [^{11}C]SN003, we found no evidence of detectable specific binding for CRF1 in vivo in baboon using PET. Our in vitro survey of human brain regions assessing the binding density or B_{max} of CRF1 indicates the amount of target protein in brain areas assessable by PET is quite low and near the limit of detectability. Moreover, we found a major species difference in binding density of the CRF1 receptor in human brain compared to baboon brain. It is possible that a B_{max} of 60–110 fmol/mg protein in human brain could be detected by a PET tracer, as has been the case for the serotonin transporter [51], but

the absence of detectable binding in the same brain regions in baboon could explain the difference in our results between in vivo studies with PET and our vitro findings. We do find some binding in baboon brain but it is due to either CRF2 or CRF-binding protein in the regions examined. Therefore, we believe that baboon is not a good species for the in vivo development of CRF1 radioligands. Yet it still may be of value to test these C-11 CRF1 radioligands in man as areas such as cerebellum may have detectable CRF1 binding by PET.

Acknowledgements

This study was supported by NIMH grant MH066620 (P.I.: J. S. Dileep Kumar). The authors are grateful for the work of the imaging team in the Division of Neuroscience and Virginia Johnson for her assistance with the autoradiography images.

References

[1]. Vale W, Spiess J, Rivier C, Rivier J. Characterization of a 41-residue ovine hypothalamic peptide that stimulates secretion of corticotropin and beta-endorphin. Science 1981;213:1394–1397. [PubMed: 6267699]

[2]. De Souza EB. Corticotropin-releasing factor receptors: physiology, pharmacology, biochemistry and role in central nervous system and immune disorders. Psychoneuroendocrinology 1995;20:789–819. [PubMed: 8834089]

[3]. Behan DP, Grigoriadis DE, Lovenberg T, Chalmers D, Heinrichs S, Liaw C, et al. Neurobiology of corticotropin releasing factor (CRF) receptors and CRF-binding protein: implications for the treatment of CNS disorders. Mol Psychiatry 1996;1:265–277. [PubMed: 9118350]

[4]. Behan DP, De Souza EB, Lowry PJ, Potter E, Sawchenko P, Vale WW. Corticotropin releasing factor (CRF) binding protein: a novel regulator of CRF and related peptides. Front Neuroendocrinol 1995;16:362–382. [PubMed: 8557170]

[5]. Grigoriadis DE, Lovenberg TW, Chalmers DT, Liaw C, De Souze EB. Characterization of corticotropin-releasing factor receptor subtypes. Ann N Y Acad Sci 1996;780:60–80. [PubMed: 8602740]

[6]. Heinrichs SC, De Souza EB, Schulteis G, Lapsansky JL, Grigoriadis DE. Brain penetrance, receptor occupancy and antistress in vivo efficacy of a small molecule corticotropin releasing factor type I receptor selective antagonist. Neuropsychopharmacology 2002;27:194–202. [PubMed: 12093593]

[7]. Chalmers DT, Lovenberg TW, Grigoriadis DE, Behan DP, De Souza EB. Corticotrophin-releasing factor receptors: from molecular biology to drug design. Trends Pharmacol Sci 1996;17:166–172. [PubMed: 8984745]

[8]. Hiroi N, Wong ML, Licinio J, Park C, Young M, Gold PW, et al. Expression of corticotropin releasing hormone receptors type I and type II mRNA in suicide victims and controls. Mol Psychiatry 2001;6:540–546. [PubMed: 11526468]

[9]. Sanchez MM, Young LJ, Plotsky PM, Insel TR. Autoradiographic and in situ hybridization localization of corticotropin-releasing factor 1 and 2 receptors in nonhuman primate brain. J Comp Neurol 1999;408:365–377. [PubMed: 10340512]

[10]. Aguilera G, Nikodemova M, Wynn PC, Catt KJ. Corticotropin releasing hormone receptors: two decades later. Peptides 2004;25:319–329. [PubMed: 15134857]

[11]. Banki CM, Bissette G, Arato M, O'Connor L, Nemeroff CB. CSF corticotropin-releasing factor-like immunoreactivity in depression and schizophrenia. Am J Psychiatry 1987;144:873–877. [PubMed: 3496802]

[12]. Nemeroff CB, Widerlov E, Bissette G, Walleus H, Karlsson I, Eklund K, et al. Elevated concentrations of CSF corticotropin-releasing factor-like immunoreactivity in depressed patients. Science 1984;226:1342–1344. [PubMed: 6334362]

[13]. Geracioti TD Jr, Loosen PT, Orth DN. Low cerebrospinal fluid corticotropin-releasing hormone concentrations in eucortisolemic depression. Biol Psychiatry 1997;42:165–174. [PubMed: 9232208]

[14]. Bremner JD, Licinio J, Darnell A, Krystal JH, Owens MJ, Southwick SM, et al. Elevated CSF corticotropin-releasing factor concentrations in posttraumatic stress disorder. Am J Psychiatry 1997;154:624–629. [PubMed: 9137116]

[15]. Chappell P, Leckman J, Goodman W, Bissette G, Pauls D, Anderson G, et al. Elevated cerebrospinal fluid corticotropin-releasing factor in Tourette's syndrome: comparison to obsessive compulsive disorder and normal controls. Biol Psychiatry 1996;39:776–783. [PubMed: 8731518]

[16]. Kaye WH, Gwirtsman HE, George DT, Ebert MH, Jimerson DC, Tomai TP, et al. Elevated cerebrospinal fluid levels of immunoreactive corticotropin-releasing hormone in anorexia nervosa: relation to state of nutrition, adrenal function, and intensity of depression. J Clin Endocrinol Metab 1987;64:203–208. [PubMed: 3491830]

[17]. Arato M, Banki CM, Bissette G, Nemeroff CB. Elevated CSF CRF in suicide victims. Biol Psychiatry 1989;25:355–359. [PubMed: 2536563]

[18]. Traskman-Bendz L, Ekman R, Regnell G, Ohman R. HPA-related CSF neuropeptides in suicide attempters. Eur Neuropsychopharmacol 1992;2:99–106. [PubMed: 1378770]

[19]. Brunner J, Stalla GK, Stalla J, Uhr M, Grabner A, Wetter TC, et al. Decreased corticotropin-releasing hormone (CRH) concentrations in the cerebrospinal fluid of eucortisolemic suicide attempters. J Psychiatr Res 2001;35:1–9. [PubMed: 11287050]

[20]. Westrin A, Ekman R, Regnell G, Traskman-Bendz L. A follow up study of suicide attempters: increase of CSF-somatostatin but no change in CSF-CRH. Eur Neuropsychopharmacol 2001;11:135–143. [PubMed: 11313159]

[21]. Austin MC, Janosky JE, Murphy HA. Increased corticotropin-releasing hormone immunoreactivity in monoamine-containing pontine nuclei of depressed suicide men. Mol Psychiatry 2003;8:324–332. [PubMed: 12660805]

[22]. Merali Z, Du L, Hrdina P, Palkovits M, Faludi G, Poulter MO, et al. Dysregulation in the suicide brain: mRNA expression of corticotropin-releasing hormone receptors and GABA(A) receptor subunits in frontal cortical brain region. J Neurosci 2004;24:1478–1485. [PubMed: 14960621]

[23]. Nemeroff CB, Owens MJ, Bissette G, Andorn AC, Stanley M. Reduced corticotropin releasing factor binding sites in the frontal cortex of suicide victims. Arch Gen Psychiatry 1988;45:577–579. [PubMed: 2837159]

[24]. McCarthy JR, Heinrichs SC, Grigoriadis DE. Recent advances with the CRF1 receptor: design of small molecule inhibitors, receptor subtypes and clinical indications. Curr Pharm Des 1999;5:289–315. [PubMed: 10213797]

[25]. Holsboer F. The rationale for corticotropin-releasing hormone receptor (CRH-R) antagonists to treat depression and anxiety. J Psychiatr Res 1999;33:181–214. [PubMed: 10367986]

[26]. Keck ME, Welt T, Wigger A, Renner U, Engelmann M, Holsboer F, et al. The anxiolytic effect of the CRH(1) receptor antagonist R121919 depends on innate emotionality in rats. Eur J Neurosci 2001;13:373–380. [PubMed: 11168542]

[27]. Zobel AW, Nickel T, Kunzel HE, Ackl N, Sonntag A, Ising M, et al. Effects of the high-affinity corticotropin-releasing hormone receptor 1 antagonist R121919 in major depression: the first 20 patients treated. J Psychiatr Res 2000;34:171–181. [PubMed: 10867111]

[28]. Hsin LW, Webster EL, Chrousos GP, Gold PW, Eckelman WC, Contoreggi C, et al. Synthesis and biological activity of fluoro-substituted pyrrolo[2,3-d]pyrimidines: the development of potential positron emission tomography imaging agents for the corticotropin-releasing hormone type 1 receptor. Bioorg Med Chem Lett 2000;10:707–710. [PubMed: 10782669]

[29]. Hsin LW, Tian X, Webster EL, Coop A, Caldwell TM, Jacobson AE, et al. CRHR1 Receptor binding and lipophilicity of pyrrolopyrimidines, potential nonpeptide corticotropin-releasing hormone type 1 receptor antagonists. Bioorg Med Chem 2002;10:175–183. [PubMed: 11738619]

[30]. Tian X, Hsin LW, Webster EL, Contoreggi C, Chrousos GP, Gold PW, et al. The development of a potential single photon emission computed tomography (SPECT) imaging agent for the corticotropin-releasing hormone receptor type. Bioorg Med Chem Lett 2001;11:331–333. [PubMed: 11212103]

[31]. Martarello L, Kilts CD, Ely T, Owens MJ, Nemeroff CB, Camp M, et al. Synthesis and characterization of fluorinated and iodinated pyrrolopyrimidines as PET/SPECT ligands for the CRF1 receptor. Nucl Med Biol 2001;28:187–195. [PubMed: 11295429]

[32]. Jagoda E, Contoreggi C, Lee MJ, Kao CH, Szajek LP, Listwak S, et al. Autoradiographic visualization of corticotropin releasing hormone type 1 receptors with a nonpeptide ligand: synthesis of [(76)Br]MJL-1-109-2. J Med Chem 2003;46:3559–3562. [PubMed: 12904058]

[33]. Kumar JS, Majo VJ, Sullivan GM, Prabhakaran J, Simpson NR, Van Heertum RL, et al. Synthesis and *in vivo* evaluation of [^{11}C]SN003: A potential PET ligand for CRF_1 receptors. Bioorganic & Medicinal Chemistry 2006;14:4029–4034. [PubMed: 16529935]

[34]. Wong DF, Pomper MG. Predicting the success of a radiopharmaceutical for in vivo imaging of central nervous system neuroreceptor systems. Mol Imaging Biol 2003;5:350–362. [PubMed: 14667490]

[35]. Kumar JS, Majo VJ, Prabhakaran J, Simpson NR, Van Heertum RL, Mann JJ. Synthesis of [N-methyl-11C]-3-[(6-dimethylamino)pyridin-3-yl]-2,5-dimethyl-N,N-dipropylpyrazolo[1,5-a] pyrimidine-7-amine: A potential PET ligand for CRF1 receptors. J Label Compd Radiopharm 2003;46:1055–1065.

[36]. Kumar JS, Majo VJ, Simpson NR, Prabhakaran J, Van Heertum RL, Mann JJ. Synthesis of [O-methyl-11C]-4-(1,3-dimethoxy-2-propylamino)-2,7-dimethyl-8-(2,4-dichlorophenyl)[1,5-a] pyrazolo-1,3,5-triazine (11C]DMP696): A potential PET ligand for CRF1 receptors. J Label Compd Radiopharm 2004;47:971–976.

[37]. Parsey RV, Ojha A, Ogden RT, Erlandsson K, Kumar D, Landgrebe M, et al. Metabolite considerations in the in vivo quantification of serotonin transporters using 11C-DASB and PET in humans. J Nucl Med 2006;47:1796–1802. [PubMed: 17079812]

[38]. Woods RP, Grafton ST, Holmes CJ, Cherry SR, Mazziotta JC. Automated image registration: I. General methods and intrasubject, intramodality validation. J Comput Assist Tomogr 1998;22:139–152. [PubMed: 9448779]

[39]. Woods RP, Grafton ST, Watson JD, Sicotte NL, Mazziotta JC. Automated image registration: II. Intersubject validation of linear and nonlinear models. J Comput Assist Tomogr 1998;22:153–165. [PubMed: 9448780]

[40]. Parsey RV, Ogden RT, Mann JJ. Determination of volume of distribution using likelihood estimation in graphical analysis: elimination of estimation bias. J Cereb Blood Flow Metab 2003;23:1471–1478. [PubMed: 14663343]

[41]. Mintun MA, Raichle ME, Martin WR, Herscovitch P. Brain oxygen utilization measured with O-15 radiotracers and positron emission tomography. J Nucl Med 1984;25:177–187. [PubMed: 6610032]

[42]. Frey KA, Hichwa RD, Ehrenkaufer RL, Agranoff BW. Quantitative in vivo receptor binding III: Tracer kinetic modeling of muscarinic cholinergic receptor binding. Proc Natl Acad Sci U S A 1985;82:6711–6715. [PubMed: 3876561]

[43]. Rominger DH, Rominger CM, Fitzgerald LW, Grzanna R, Largent BL, Zaczek R. Characterization of [125I]sauvagine binding to CRH2 receptors: membrane homogenate and autoradiographic studies. J Pharmacol Exp Ther 1998;286:459–468. [PubMed: 9655891]

[44]. Zhang G, Huang N, Li YW, Qi X, Marshall AP, Yan XX, et al. Pharmacological characterization of a novel nonpeptide antagonist radioligand, (+/−)-N-[2-methyl-4-methoxyphenyl]-1-(1-(methoxymethyl)propyl)-6-methyl-1H-1,2,3-triazolo[4,5-c]pyridin-4-amine ([3H]SN003) for corticotropin-releasing factor1 receptors. J Pharmacol Exp Ther 2003;305:57–69. [PubMed: 12649353]

[45]. Li YW, Hill G, Wong H, Kelly N, Ward K, Pierdomenico M, et al. Receptor occupancy of nonpeptide corticotropin-releasing factor 1 antagonist DMP696: correlation with drug exposure and anxiolytic efficacy. J Pharmacol Exp Ther 2003;305:86–96. [PubMed: 12649356]

[46]. Millan MA, Jacobowitz DM, Hauger RL, Catt KJ, Aguilera G. Distribution of corticotropin-releasing factor receptors in primate brain. Proc Natl Acad Sci U S A 1986;83:1921–1925. [PubMed: 2869491]

[47]. Kostich WA, Grzanna R, Lu NZ, Largent BL. Immunohistochemical visualization of corticotropin-releasing factor type 1 (CRF1) receptors in monkey brain. J Comp Neurol 2004;478:111–125. [PubMed: 15349973]

[48]. Primus RJ, Yevich E, Baltazar C, Gallager DW. Autoradiographic localization of CRF1 and CRF2 binding sites in adult rat brain. Neuropsychopharmacology 1997;17:308–316. [PubMed: 9348546]

[49]. Hoare SR, Sullivan SK, Ling N, Crowe PD, Grigoriadis DE. Mechanism of corticotropin-releasing factor type I receptor regulation by nonpeptide antagonists. Mol Pharmacol 2003;63:751–765. [PubMed: 12606786]

[50]. Tokugawa J, Ravasi L, Nakayama T, Lang L, Schmidt KC, Seidel J, et al. Distribution of the 5-HT (1A) receptor antagonist [(18)F]FPWAY in blood and brain of the rat with and without isoflurane anesthesia. European journal of nuclear medicine and molecular imaging 2007;34:259–266. [PubMed: 17021813]

[51]. Zeng Z, Chen TB, Miller PJ, Dean D, Tang YS, Sur C, et al. The serotonin transporter in rhesus monkey brain: comparison of DASB and citalopram binding sites. Nucl Med Biol 2006;33:555–563. [PubMed: 16720249]

[52]. He L, Gilligan PJ, Zaczek R, Fitzgerald LW, McElroy J, Shen HS, et al. 4-(1,3- Dimethoxyprop-2-ylamino)-2,7-dimethyl-8-(2, 4-dichlorophenyl)pyrazolo[1,5-a]-1,3,5-triazine: a potent, orally bioavailable CRF(1) receptor antagonist. J Med Chem 2000;43:449–456. [PubMed: 10669572]

[53]. Mackay KB, Bozigian H, Grigoriadis DE, Loddick SA, Verge G, Foster AC. Neuroprotective effects of the CRF1 antagonist R121920 after permanent focal ischemia in the rat. J Cereb Blood Flow Metab 2001;21:1208–1214. [PubMed: 11598498]

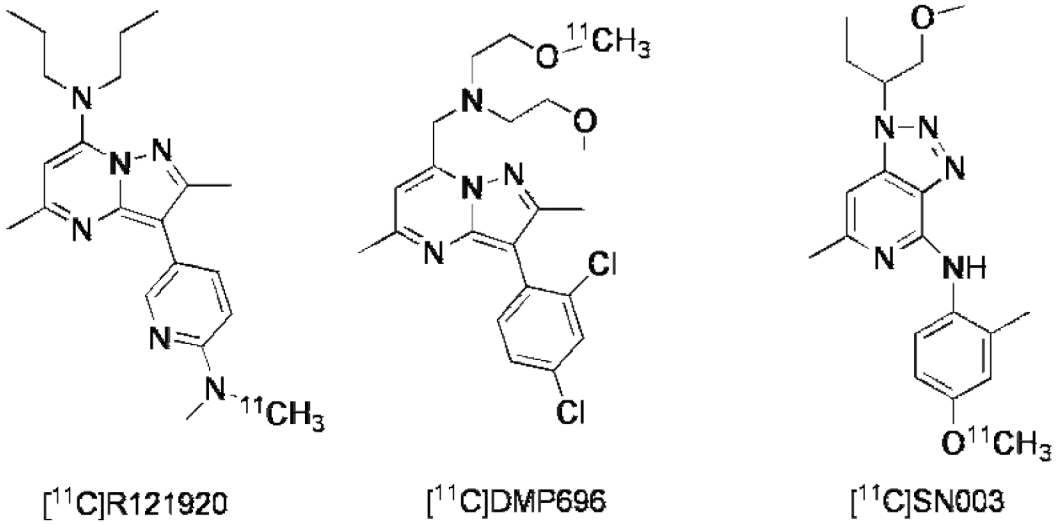

Figure 1.
Structures of radioligands. **A**) [^{11}C]R121920. **B**) [^{11}C]DMP696. **C**) [^{11}C]SN003.

A) Metabolism Curve for [^{11}C]R121920

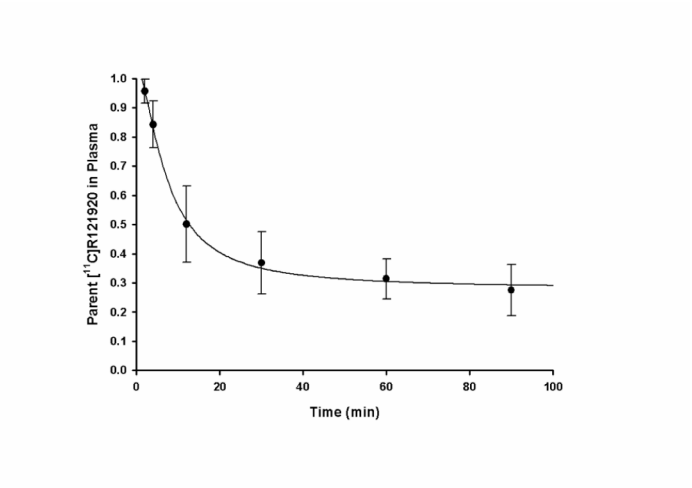

B) Metabolism Curve for [^{11}C]DMP696

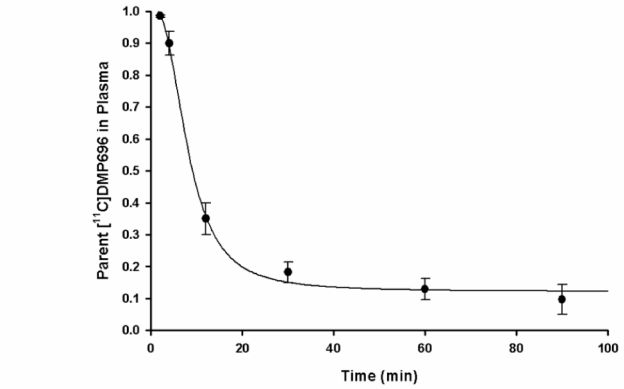

Figure 2.

Unmetabolized parent fractions of the radioligands over time in baboon plasma. **A**) Fraction of [^{11}C]R121920. **B**) Fraction of [^{11}C]DMP696. Filled circles represent mean fractions in six determinations and error bars represent standard deviations.

A) Time-Activity Curve for [^{11}C]R121920

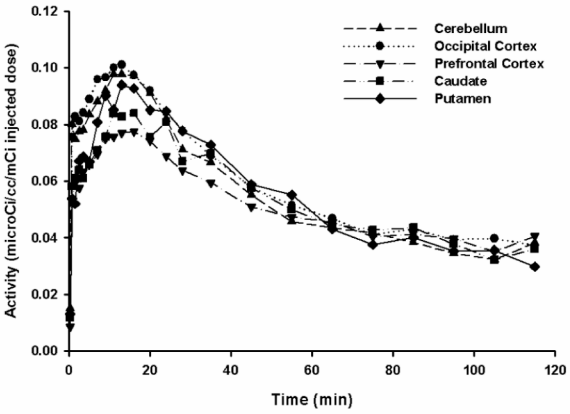

B) Time-Activity Curve for [^{11}C]DMP696

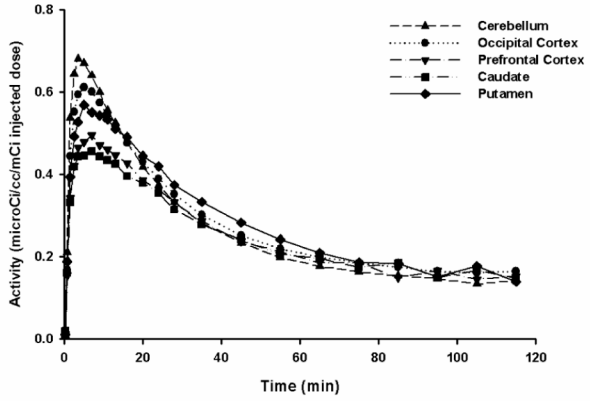

Figure 3.
Time-activity curves of the radioactivity in selected regions of interest in baboon brain during PET imaging. **A**) Time-activity curve of [^{11}C]R121920. **B**) Time-activity curve of [^{11}C] DMP696.

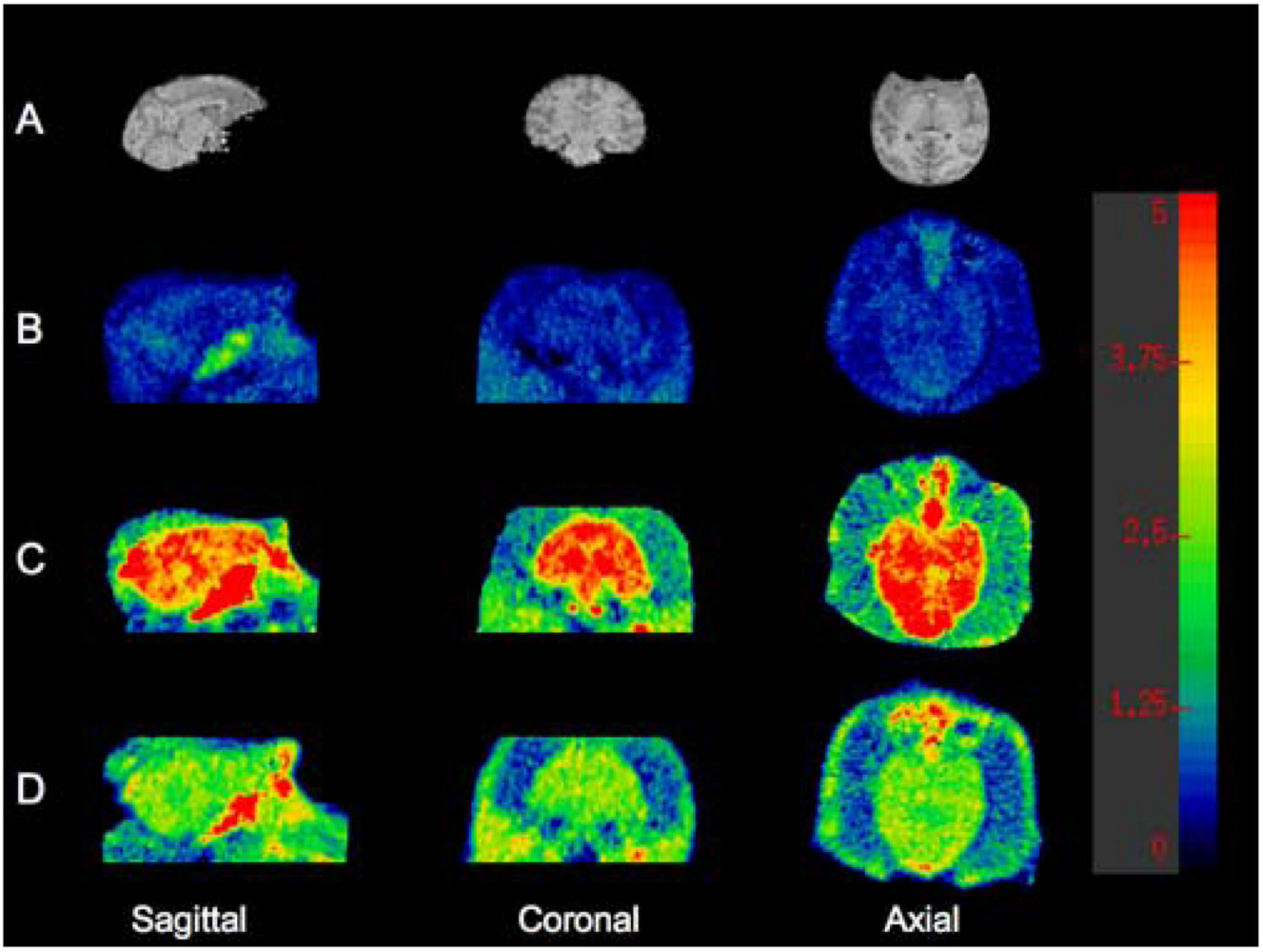

Figure 4.

Representative volume of distribution (V_T) voxel maps of C-11 CRF1 radioligands in the same baboon from 120 min emission scans performed under isoflurane anesthesia. Intensity bar shows corresponding V_T values for each intensity level. **A**) Cropped saggital, coronal, and axial magnetic resonance imaging (MRI) images of baboon. **B**) V_T voxel map of [^{11}C]R121920 (injected dose [ID], 4.1 mCi; specific activity [SA], 1.8 Ci/micromole). **C**) V_T voxel map of [^{11}C]DMP696 (ID, 4.0 mCi; SA, 2.2 Ci/micromole). **D**) V_T voxel map of previously reported CRF1 radioligand [^{11}C]SN003 (ID, 4.7 mCi; SA, 2.1 Ci/micromole).

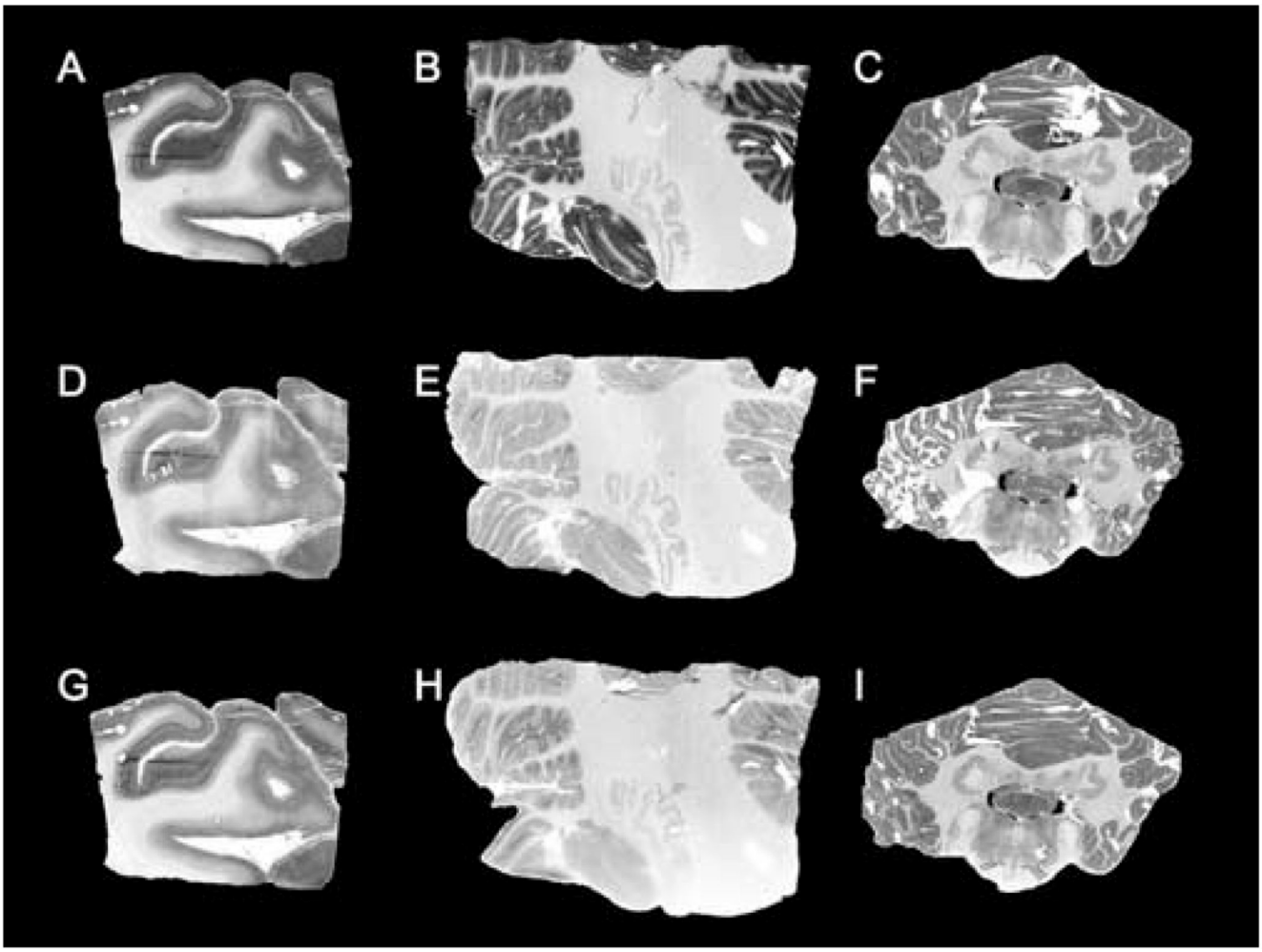

Figure 5.

Representative autoradiography images of [^{125}I]Tyr^{0}-sauvagine binding to selected regions of human and baboon brain. **A**) Total binding in human occipital cortex (OC). **B**) Total binding in human cerebellum (CER). **C**) Total binding in baboon cerebellum. **D**) Nonspecific (NS) binding in human OC with CP154,526 as displacer. **E**) NS binding in human CER with CP154,526 as displacer. **F**) NS binding in baboon CER with CP154,526 as displacer. **G**) NS binding in human OC with SN003 as displacer. **H**) NS binding in human CER with SN003 as displacer. **I**) NS binding in baboon CER with SN003 as displacer.

Table 1.

Chemical Characteristics of the CRF1 Radioligands

Radioligand	Molecular Weight	Calculated Log *P* Value	K_i (nM)[b]	Synthesis Time (min)	Yield (%)[c]	SA (Ci/μmol)[d]
[^{11}C]R121920	367	4.0[a]	4.0	30	5	>1000
[^{11}C]DMP696	410	3.2[e]	1.7	30	25	>2000
[^{11}C]SN003	356	3.1[e]	4.0	30	22	>2000

[a] Calculated with ACD/ log*P* DB program

[b] Of the unlabeled antagonist [44,52,53]

[c] At the end of synthesis (EOS)

[d] SA = specific activity measured at end of bombardment (EOB)

[e] Determined by shake-flask method

Table 2.

Volume of Distribution (V_T) for Selected Regions for the CRF1 Radioligands

	Volume of Distribution (V_T; ml/g)		
Ligand	**Putamen**	**Occipital Cortex**	**Cerebellum**
[^{11}C]R121920	1.5 ± 0.4	1.5 ± 0.3	1.4 ± 0.4
[^{11}C]DMP696	5.5 ± 0.6	5.5 ± 0.5	5.0 ± 0.6
[^{11}C]SN003	4.2 ± 0.6	4.5 ± 0.6	4.6 ± 0.7